

基于柔性苯二乙酸构筑的三个钴配合物的晶体结构和电化学性质

张美丽* 郑艳金 刘 敏 任宜霞 王记江 崔华莉 刘 琳
(延安大学化学与化工学院, 陕西省化学反应工程重点实验室, 延安 716000)

摘要: 利用水热法合成了 3 个钴配位聚合物 $\{[\text{Co}_{1.5}(\text{opda})_{1.5}(\text{mbib})_2(\text{H}_2\text{O})_2] \cdot \text{H}_2\text{O}\}_n$ (**1**), $\{[\text{Co}(\text{mpda})(\text{mbib})] \cdot \text{H}_2\text{O}\}_n$ (**2**) 和 $\{[\text{Co}(\text{ppda})(\text{mbib})] \cdot \text{H}_2\text{O}\}_n$ (**3**), 并对其进行了元素分析、红外光谱、热重分析和 X 射线单晶衍射测定。结果表明这些配合物的不同结构主要是由于中心钴(II)阳离子的配位几何结构、柔性苯二甲酸和双(咪唑)配体的配位方式和构象的不同。同时, 还研究了 3 个钴配位聚合物的热稳定性和电化学性质。

关键词: 配位聚合物; 晶体结构; 电化学性质

中图分类号: O614.81+2

文献标识码: A

文章编号: 1001-4861(2019)10-1813-08

DOI: 10.11862/CJIC.2019.214

Crystal Structures and Electrochemistry Properties of Three Co(II) Complexes Based on Flexible Phenylenediacetate Ligands

ZHANG Mei-Li* ZHENG Yan-Jin LIU Min REN Yi-Xia WANG Ji-Jiang CUI Hua-Li LIU Lin
(Department of Chemistry and Chemical Engineering, Shaanxi Key Laboratory of Chemical Reaction Engineering, Yan'an University, Yan'an, Shaanxi 716000, China)

Abstract: Three new coordination complexes, $\{[\text{Co}_{1.5}(\text{opda})_{1.5}(\text{mbib})_2(\text{H}_2\text{O})_2] \cdot \text{H}_2\text{O}\}_n$ (**1**), $\{[\text{Co}(\text{mpda})(\text{mbib})] \cdot \text{H}_2\text{O}\}_n$ (**2**) and $\{[\text{Co}(\text{ppda})(\text{mbib})] \cdot \text{H}_2\text{O}\}_n$ (**3**) (H_2opda =1,2-phenylenediacetic acid, H_2mpda =1,3-phenylenediacetic acid, H_2ppda =1,4-phenylenediacetic acid, mbib =1,3-bis(1-imidazolyl)benzene), have been synthesized by using cobalt salt and bis (imidazole) ligand in the presence of different flexible phenylenediacetate blocks under hydrothermal conditions, and characterized by elemental analysis, IR spectroscopy and single-crystal X-ray crystallography. Single-crystal X-ray diffraction analysis revealed that the diverse structures of these complexes are mainly attributed to various coordination geometries of the central cobalt (II) cations, coordination modes and conformations of the flexible phenylenediacetic acid and bis (imidazole) ligands. Furthermore, thermal gravimetric analysis (TGA) and the electrochemistry properties of **1~3** are also investigated, and all of them have good cyclic voltammograms. CCDC: 1856259, **1**; 1856260, **2**; 1856261, **3**.

Keywords: coordination polymer; crystal structure; electrochemistry property

0 Introduction

The rational design and synthesis of polymeric metal-organic hybrid complexes has been extensively

studied in recent years, not only on their intriguing structural diversity^[1], but also on their intrinsic aesthetic appeal and encouraging properties such as catalysis^[2], luminescence^[3-7], chemical sensing^[8], energy

收稿日期: 2019-04-12。收修改稿日期: 2019-08-02。

国家自然科学基金(No.21573189), 陕西省教育厅专项科学研究计划(No.19JK0966), 延安大学科研计划(No.YDQ2017-12)和陕西省大学生创新训练(No.S201910719058)资助项目。

*通信联系人。E-mail: ydzml2332041@163.com, Tel(Fax): 0911-2332037; 会员登记号: S06N0331M1005。

storage conversion^[9], and drug delivery^[10-11]. To date, it is still a challenge to predict the exact structure of assembly products in crystal engineering since the structure is mainly dependent by many factors such as the coordination geometries of the metal centers, the coordination behaviours of the organic building blocks, and guest solvent or counter ions^[12].

Among the reported studies, organic aromatic polycarboxylate ligands have attracted intensive research interest due to their various coordination modes to metal ions, resulting from completely or partially deprotonated sites allowing for the large diversity of topologies^[13]. In contrast to those of rigid ligands, the backbone flexibility and conformation changeability afford these flexible ligands versatile bridging modes and make the structures of their coordination polymers more diversiform and more difficult to predict^[14-15]. However, it is still a challenge to understanding the control of structure and topology of coordination polymers. In our recent work, a series of coordination polymers based on flexible phenylenediacetate and different bis (imidazole) ligands have been successfully obtained^[16-17], and we are systematically investigating the influence of the coordination chemistry of phenylenediacetate ligands with different coordination groups, conformations, and flexibility. As a continuation of our research, by employing the mixture of different flexible phenylenediacetate building blocks in the presence of bis(imidazole) ligand 1,3-bis(1-imidazolyl)benzene (mbib), three new coordination polymers $\{[\text{Co}_{1.5}(\text{opda})_{1.5}(\text{mbib})_2(\text{H}_2\text{O})_2] \cdot \text{H}_2\text{O}\}_n$ (**1**), $\{[\text{Co}(\text{mpda})(\text{mbib})] \cdot \text{H}_2\text{O}\}_n$ (**2**) and $\{[\text{Co}(\text{ppda})(\text{mbib})] \cdot \text{H}_2\text{O}\}_n$ (**3**) (H_2opda =1,2-phenylenediacetic acid, H_2mpda =1, 3-phenylenediacetic acid, H_2ppda =1, 4-phenylenediacetic acid, showing structural diversities have been synthesized and structurally characterized. Furthermore, their thermal gravimetric analysis (TGA) and electrochemistry properties have also been investigated.

1 Experimental

1.1 Materials and methods

All the starting reagents and solvents were

commercially available and used as received without further purification. The hydrothermal reaction was performed in a 25 mL Teflon-lined stainless steel autoclave under autogenous pressure. Elemental analyses for C, H, and N were carried out on a Flash 2000 elemental analyzer. Thermal gravimetric analysis (TGA) were carried out on a SDT Q600 thermogravimetric analyzer. A platinum pan was used for heating the sample with a heating rate of $10\text{ }^\circ\text{C} \cdot \text{min}^{-1}$ under a N_2 atmosphere. Powder X-ray diffraction (PXRD) measurements were performed on a Bruker D8-ADVANCE X-ray diffractometer with $\text{Cu } K\alpha$ radiation ($\lambda=0.154\text{ }2\text{ nm}$), and the experimental test conditions were the voltage of 40 kV, the current of 30 mA, and the scanning range of $5^\circ\sim 50^\circ$.

1.2 Syntheses of the complexes

$\{[\text{Co}_{1.5}(\text{opda})_{1.5}(\text{mbib})_2(\text{H}_2\text{O})_2] \cdot \text{H}_2\text{O}\}_n$ (**1**). A mixture of H_2opda (0.009 6 g, 0.05 mmol), $\text{Co}(\text{OAc})_2 \cdot 4\text{H}_2\text{O}$ (0.024 9 g, 0.1 mmol), (0.018 6 g, 0.1 mmol) and KOH (5.6 mg, 0.1 mmol) were added to water (12 mL) in a 25 mL Teflon-lined stainless steel vessel. The mixture was heated at $150\text{ }^\circ\text{C}$ for 72 h. After the reactive mixture was slowly cooled to room temperature, violet block crystals of **1** were obtained. Elemental analysis Calcd. for $\text{C}_{78}\text{H}_{76}\text{Co}_3\text{N}_{16}\text{O}_{18}(\%)$: C 55.03, H 4.50, N 13.17; Found(%): C 55.37, H 4.25, N 13.53.

$\{[\text{Co}(\text{mpda})(\text{mbib})] \cdot \text{H}_2\text{O}\}_n$ (**2**). Complex **2** was synthesized by a procedure similar to that of **1**, except that H_2mpda (0.009 6 g, 0.05 mmol) replaced H_2opda . Violet block crystals of **2** were obtained. Elemental analysis Calcd. for $\text{C}_{44}\text{H}_{40}\text{Co}_2\text{N}_8\text{O}_{10}(\%)$: C 55.12, H 4.21, N 11.69; Found(%): C 54.89, H 4.35, N 11.37.

$\{[\text{Co}(\text{ppda})(\text{mbib})] \cdot \text{H}_2\text{O}\}_n$ (**3**). Complex **3** was synthesized by a procedure similar to that of **1**, except that H_2ppda (0.009 6 g, 0.05 mmol) replaced H_2opda . Violet block crystals of **3** were obtained. Elemental analysis Calcd. for $\text{C}_{22}\text{H}_{20}\text{CoN}_4\text{O}_5(\%)$: C 55.12, H 4.21, N 11.69; Found(%): C 55.18, H 4.29, N 11.27.

1.3 Crystal structure determination

X-ray single-crystal diffraction data for complexes **1-3** were collected on a Bruker Smart 1000 CCD area-detector diffractometer with $\text{Mo } K\alpha$ radiation ($\lambda=0.071\text{ }073\text{ nm}$) by ω scan mode. The crystal structure

was solved by direct methods, using SHELXS-2014 and least-squares refined with SHELXL-2014^[18]. Non-hydrogen atoms were refined anisotropically and hydrogen atoms were placed in geometrically calculated

positions. Further details for structural analysis are summarized in Table 1. Selected bond distances and bond angles are listed in Table S1.

CCDC: 1856259, **1**; 1856260, **2**; 1856261, **3**.

Table 1 Crystallographic data and refinement parameters for complexes **1**~**3**

Complex	1	2	3
Empirical formula	C ₇₈ H ₇₆ Co ₃ N ₁₆ O ₁₈	C ₄₄ H ₄₀ Co ₂ N ₈ O ₁₀	C ₂₂ H ₂₀ CoN ₄ O ₅
Formula weight	1 702.33	958.70	479.35
Crystal system	Triclinic	Monoclinic	Orthorhombic
Space group	$P\bar{1}$	$P2_1/n$	$Pna2_1$
<i>a</i> / nm	1.100 0(6)	0.798 5(3)	1.889 4(2)
<i>b</i> / nm	1.274 1(7)	3.794 6(14)	0.789 1(9)
<i>c</i> / nm	1.534 4(8)	1.391 5(5)	1.429 1(16)
α / (°)	103.410 0(10)		
β / (°)	108.677 0(10)	96.276 0(10)	
γ / (°)	95.755 0(10)		
<i>V</i> / nm ³	1.945 8(18)	4.190 7(3)	2.131 3(4)
<i>Z</i>	1	4	4
<i>D_c</i> / (g·cm ⁻³)	1.453	1.519	1.494
μ / mm ⁻¹	0.713	0.862	0.848
<i>R_{int}</i>	0.010 5	0.117 6	0.034 3
Goodness-of-fit on <i>F</i> ²	1.194	1.034	1.044
<i>R</i> ₁ ^a , <i>wR</i> ₂ ^b [<i>I</i> > 2σ(<i>I</i>)]	0.049 5, 0.132 3	0.061 3, 0.092 8	0.030 9, 0.069 6
<i>R</i> ₁ ^a , <i>wR</i> ₂ ^b (all data)	0.046 7, 0.131 0	0.149 7, 0.111 9	0.039 4, 0.073 0

$$^a R_1 = \sum \|F_o\| - \|F_c\| / \sum \|F_o\|; ^b wR_2 = [\sum w(F_o^2 - F_c^2)^2 / \sum w(F_o^2)^2]^{1/2}$$

2 Results and discussion

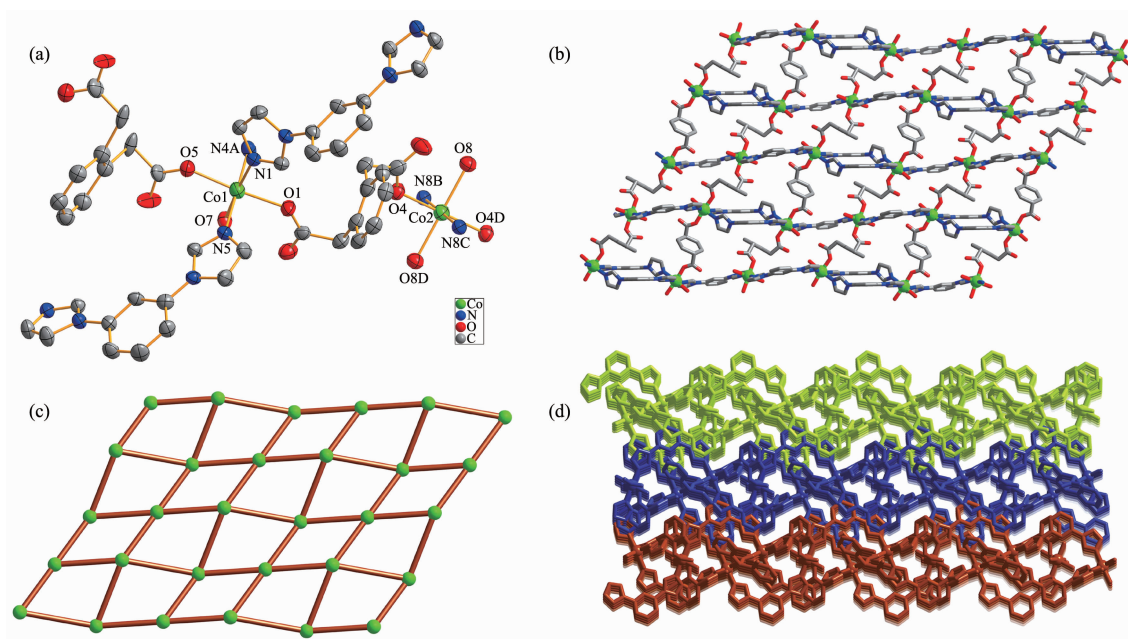
2.1 Description of crystal structure

2.1.1 Crystal structure of {[Co_{1.5}(opda)_{1.5}(mbib)₂(H₂O)₂]·H₂O}_n (**1**)

Single-crystal X-ray diffraction analysis reveals that complex **1** crystallizes in the triclinic system, $P\bar{1}$ space group, and features a 2D network. The asymmetric unit of **1** consists of one and a half of cobalt(II) ions, one and a half of fully deprotonated opda²⁻ ligands, two mbib ligands, two coordinated water molecules and one lattice water molecule. The central Co1 atom has a distorted octahedral coordination geometry, coordinated by three nitrogen atoms of three different mbib ligands (Co1-N1 0.208 3(3) nm, Co1-N4A 0.208 1(4) nm, Co1-N5 0.206 8(4) nm) and three oxygen atoms from two different opda ligands and one water molecule (Co1-O1 0.205 6(3) nm, Co1-O5

0.207 4(3) nm, Co1-O7 0.212 7(3) nm). While the Co2 central atom is six-coordinated with a distorted octahedral coordination sphere, which is formed by two nitrogen atoms of two different mbib ligands (Co2-N8B/N8C 0.206 6(4) nm) and four oxygen atoms from three different opda²⁻ ligands and one water molecule (Co2-O4/O4D 0.206 9(3) nm, Co2-O8/O8D 0.210 1(3) nm) (Fig.1a).

In the structure of **1**, there are two kinds of mbib ligand showing non-planar conformation with the dihedral angle between benzene core and imidazole arms being 69.00° and 9.04°, 23.09° and 4.88°, respectively. Thus, the two unique Co1 atoms are bridged by two mbib ligands to form a paddle-wheel [(Co1)₂(mbib)₂] loop. Adjacent ones are further connected through [Co2(mbib)₂] motif to generate a 1D loop containing polymer chain (Fig.S1). The chains are further extended by opda²⁻ in $\mu_4\text{-}\eta^1\text{-}\eta^0$ bis(monodentate)



All hydrogen atoms are omitted for clarity; Symmetry codes: A: $1-x, -y, -z$; B: $2-x, 1-y, 1-z$; C: $-1+x, -1+y, +z$; D: $1-x, -y, 1-z$

Fig.1 (a) Coordination environments of Co(II) ion in complex **1** with 30% probability displacement ellipsoids; (b) Ball-and-stick view of 2D layer in **1**; (c) Schematic view of (4,4) net in **1**; (d) View of 3D network of **1** extended by 2D layers in an offset stacking fashion

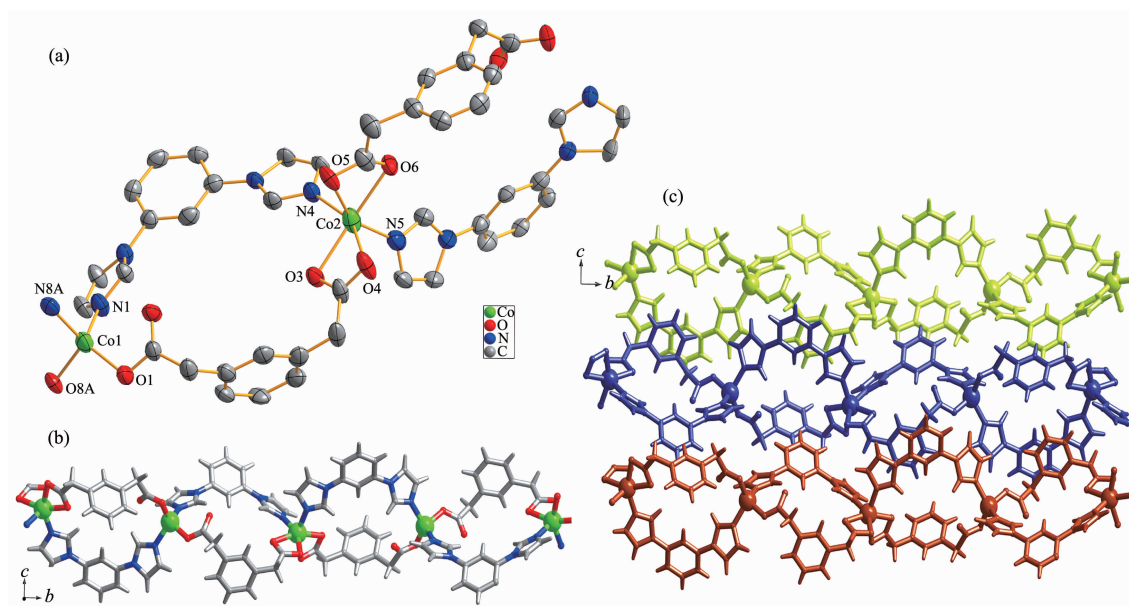
coordination modes to form a 2D (4,4) net (Fig.1b and 1c). In addition, viewed along c direction, the above-mentioned adjacent 1D chains are further interlinked to extend into an overall 3D hydrogen-bonded network (Fig.1d) by the co-effects of the inter-layer $C-H\cdots\pi$ ($C25-H25\cdots\pi$) stacking between benzene rings of mbib and $opda^{2-}$ ligands in an edge-to-face orientation with the $C\cdots\pi$ separations of 0.356 4 nm as well as $C-H\cdots O$ hydrogen-bonding interactions between benzene rings and carboxylate O atoms of $opda^{2-}$ ligands ($C24-H24\cdots O5$).

2.1.2 Crystal structure of $\{[Co(mpda)(mbib)]\cdot H_2O\}_n$ (**2**)

Utilizing the analogous bridging ligand $mpda^{2-}$, instead of the $opda^{2-}$, the 1D polymer chain of **2** was obtained. Single-crystal X-ray diffraction analysis reveals that complex **2** crystallizes in the monoclinic system, $P2_1/n$ space group, and the asymmetric unit of **2** contains two crystallographically independent Co(II) centers, each having a different coordination sphere. As shown in Fig.2a, Co1 centers adopt slightly distorted tetrahedral geometries, coordinated by two nitrogen

atoms of two mbib ligands (Co1-N1 0.204 0(2) nm, Co1-N8A 0.200 6(3) nm) and two oxygen atoms from two $mpda^{2-}$ ligands (Co1-O1 0.195 7(2) nm, Co1-O8A 0.195 5(2) nm). Co2 has a slightly distorted octahedral coordination environment, formed by four carboxyl oxygen atoms from two different $mpda^{2-}$ ligands (Co2-O3 0.218 1(2) nm, Co2-O4 0.225(3) nm, Co2-O5 0.190 1(18) nm, Co2-O6 0.225 5(2) nm) and two nitrogen atoms from two different mbib molecules (Co2-N4 0.206 0(2) nm, Co2-N5 0.208 1(3) nm).

As same as **1**, the mbib ligands in the structure of **2** also exhibit non-planar conformation with the dihedral angle between benzene core and imidazole arms of 37.36° and 15.85° , 37.12° and 37.97° , respectively. In **1**, the $opda^{2-}$ ligand has a *trans*-conformation with two carboxyl groups locating in two sides of the benzene ring plane, which can be viewed as a linear building block. Differently, the $mpda^{2-}$ ligand in **2** shows a *cis*-conformation with two carboxyl groups lying on the same sides of the benzene ring plane and acts as a “V” type building block. Thus, two kinds of such “V” type building block link the Co



All hydrogen atoms are omitted for clarity; Symmetry codes: A: $-x+1/2, y-1/2, -z+1/2$

Fig.2 (a) Coordination environments of Co(II) ion in complex **2** with 30% probability displacement ellipsoids; (b) Ball-and-stick view of 1D loop-containing chain along *b* direction in **2**; (c) View of 2D extended supramolecular layer in **2**

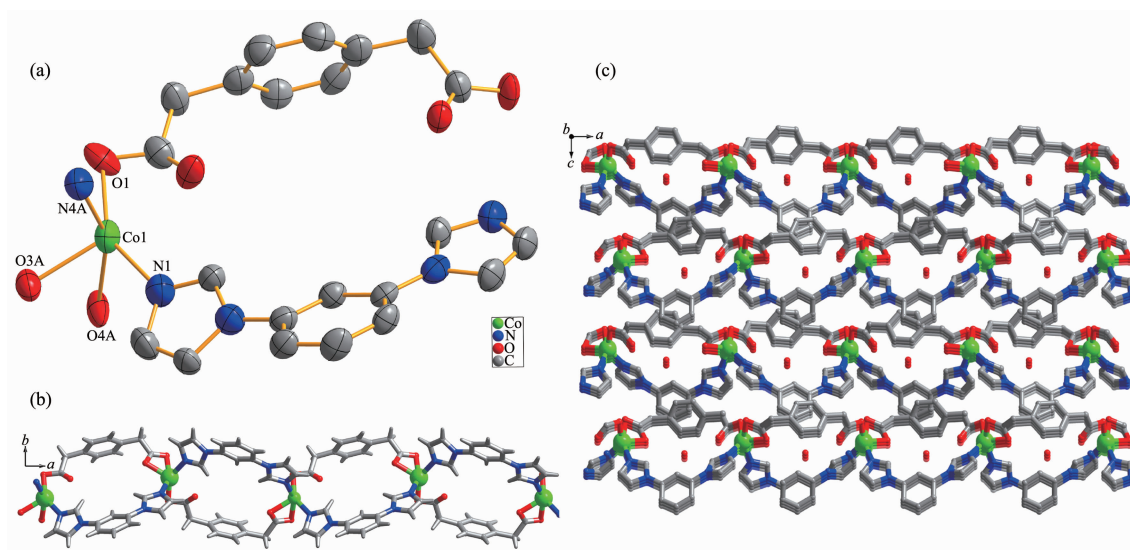
(II) ions giving rise to a 1D loop containing polymeric ribbon running along *b* direction (Fig.2b). In addition, the adjacent ribbon motifs are arranged into a 2D plane parallel to the *bc* plane by the co-effects of the inter-layer C–H $\cdots\pi$ (C43–H43 $\cdots\pi$) stacking between benzene ring of mbib and methyl of mpda²⁻ ligand in an edge-to-face orientation with the C $\cdots\pi$ separations of 0.407 3 nm as well as C–H \cdots O hydrogen-bonding interactions between imidazole rings of mbib and carboxylate O atoms of mpda²⁻ ligands (C24–H24 \cdots O1, C24 \cdots O1 0.321 5 nm).

2.1.3 Crystal structure of $\{[\text{Co}(\text{ppda})(\text{mbib})]\cdot\text{H}_2\text{O}\}_n$ (**3**)

When the ppda²⁻ building block was used, the similar 1D polymeric ribbon of **3** can also be isolated. Single crystal X-ray structure analysis reveals that the asymmetric unit of **3** contains one Co(II) ion, one fully deprotonated ppda²⁻ ligand, one mbib ligand and one lattice water molecule. As shown in Fig.3a, unlike in **1** and **2**, each Co(II) ion in **3** is penta-coordinated by two N-atom donors from two mbib ligands (Co1–N1 0.205 2(3) nm, Co1–N4A 0.204 7(3) nm) and three O atoms from two different ppda²⁻ ligands (Co1–O1

0.220 4 (18) nm, Co1–O3A 0.212 8 (3) nm, Co1–O4A 0.204 7(3) nm).

In the structure of **3**, the dihedral angle between two imidazole arms and benzene core is 32.91° and 14.22°, respectively. Two carboxyl groups of ppda²⁻ in **3** adopt monodentate and chelate coordination mode and point to the same side of the benzene ring plane. Thus, the ppda²⁻ ligand also has a *cis*-conformation and can be seen as a “V” type building block. Co(II) ions are joined together to form a 1D loop containing polymeric ribbon running along *a* direction (Fig.3b) by the mixture of two “V” type building block: mbib and ppda²⁻ ligands. The Co \cdots Co separation through mbib ligand in **3** (0.957 5 nm) is close to those in **2** (0.950 3 and 0.969 3 nm) and shorter than that in **1** (1.090 4 nm). The crystal packing diagram of **3** shows that the adjacent 1D polymeric ribbon motif are bound together by strong intermolecular hydrogen bonds to create a 2D supramolecular layer (Fig.S2). The hydrogen bonding system in **3** consists of the C–H \cdots O (C2 \cdots O4 0.363 2 nm, \angle C2–H2B \cdots O4=163.18°) hydrogen bonding interactions between methyl of ppda²⁻ from ribbon and carboxylate O atoms from the other ppda²⁻. In



All hydrogen atoms are omitted for clarity; Symmetry code: A: $x-1/2, -y+3/2, z$

Fig.3 (a) Coordination environments of Co(II) ion in complex **3** with 30% probability displacement ellipsoids; (b) Ball-and-stick view of 1D loop-containing chain along *a* direction in **3**; (c) View of 3D porous supramolecular network in **3** with lattice molecules in the channel

addition, the extended 3D porous supramolecular network (Fig.3c) is formed through $\pi \cdots \pi$ interactions (centroid-centroid distance 0.397 5 nm) between benzene rings of ppda²⁻ and mbib ligands with a face-to-face orientation. The lattice water molecules are fixed in the channels through C–H \cdots O (C13 \cdots O5 0.348 4 nm, \angle C13–H13 \cdots O5=170.49°; C17 \cdots O5 0.336 1 nm, \angle C17–H17 \cdots O5=163.1843°; C23 \cdots O5 0.352 6 nm, \angle C23–H123 \cdots O5=153.95°) and O–H \cdots O (O5 \cdots O2 0.294 4 nm, \angle O5–H5A \cdots O2=151.73°; O5 \cdots O3 0.338 3 nm, \angle O5–H5B \cdots O3=146.26°) hydrogen bonding interactions. There is no doubt that these strong hydrogen-bonding interactions play an important role in the formation of the 3D supramolecular architecture.

2.2 PXRD results and thermal analysis of complexes 1~3

In order to confirm the phase purity of the bulk materials, powder X-ray diffraction (PXRD) patterns of complexes **1**~**3** were recorded at room temperature. As shown in Fig.S3, the peak positions of the experimental PXRD and computer-simulated patterns are in agreement with each other, which confirms its phase purity. The difference in intensity of some diffraction peaks may be attributed to the preferred

orientation of the crystalline powder samples. To examine the stability of these complexes, thermal gravimetric analysis (TGA) experiment was performed. As shown in Fig.4, the TGA curves exhibit a weight loss of 5.9% (95~208 °C) for **1**, 3.3% (80~130 °C) for **2**, and 3.5% (78~135 °C) for **3**, corresponding to the release of coordinated water molecules and/or free water molecules (Calcd. 6.1%, 3.7%, and 3.7% for **1**~**3**, respectively). The skeleton of **1**~**3** can be stable up to 267, 300 and 311 °C, respectively.

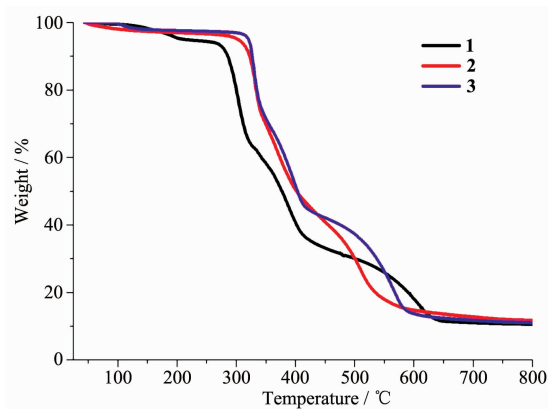


Fig.4 Thermal gravimetric analysis (TGA) curves of complexes **1**~**3**

2.3 Electrochemistry properties

In the cyclic voltammetry (CV) measurement of complexes, we employed a conventional three-

electrodes system where a saturated calomel electrode (SCE) as the reference electrode, platinum electrodes as auxiliary electrode, and foam nickel electrode was chosen as the working electrode. Water was used as solvent, and the supporting electrolyte was $1 \text{ mol} \cdot \text{L}^{-1}$ KOH solution. Cyclic voltammograms of complexes **1**~**3** are shown in Fig.5. During scanning from -0.5 to 0.5 V in a rate of $100 \text{ mV} \cdot \text{s}^{-1}$, the cyclic voltammogram curves had an oxidation-reduction peak, which corresponds to Co(II)/Co(I) redox process^[19-21]. The cyclic voltammograms of complexes **1**, **2** and **3** all showed a reversible redox wave, and the observed potential were as follows: $E_{1/2}=0.258 \text{ V}$ ($\Delta E_p=0.089 \text{ V}$) for **1**, $E_{1/2}=0.202 \text{ V}$ ($\Delta E_p=0.091 \text{ V}$) for **2**, $E_{1/2}=0.178 \text{ V}$ ($\Delta E_p=0.105 \text{ V}$) for **3**. For complexes **1**~**3**, their electrochemical behaviors are similar except for some slight potential shifts, due to the similarity of the different ligands that make up the three complexes.

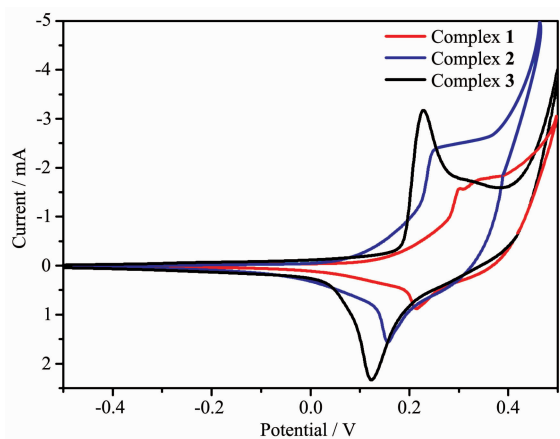


Fig.5 Cyclic voltammograms of complexes **1**~**3**

3 Conclusions

In summary, three new coordination polymers $\{[\text{Co}_{1.5}(\text{opda})_{1.5}(\text{mbib})_2(\text{H}_2\text{O})_2] \cdot \text{H}_2\text{O}\}_n$ (**1**), $\{[\text{Co}(\text{mpda})(\text{mbib})] \cdot \text{H}_2\text{O}\}_n$ (**2**) and $\{[\text{Co}(\text{ppda})(\text{mbib})] \cdot \text{H}_2\text{O}\}_n$ (**3**) have been synthesized under hydrothermal conditions by the reaction of Co(II) salt and bis(imidazole) ligand in the presence of different flexible phenylenediacetate blocks. In these complexes, the central Co(II) ions show different coordination geometries, the opda^{2-} ligand exhibits *trans*-conformation and acts as bridging building block to extend 1D loop containing $(\text{Co}-\text{mbib})$ polymer chain into a 2D network in **1**. While mpda^{2-}

and ppda^{2-} ligands in **2** and **3** possesses *cis*-conformation and can be seen as “V” type building block, linking Co(II) ions to form 1D loop containing chain together with *mbib* ligand. The structural diversities of these complexes are significantly affected by the coordination geometries of the central metal ions and the coordination modes, conformations of the organic ligands. All of three complexes are electrochemically active. This study is significant for extending the metal-organic complexes containing electronic conjugated system, exploring the interrelation between structure and property to develop potential electrochemical functional materials.

Supporting information is available at <http://www.wjhxsb.cn>

References:

- [1] Li D S, Wu Y P, Zhao J, et al. *Coord. Chem. Rev.*, **2014**,**261**: 1-27
- [2] Zhao Y, Deng D S, Ma L F, et al. *Chem. Commun.*, **2013**,**49**: 10299-10301
- [3] Hu Z, Deibert B J, Li J. *Chem. Soc. Rev.*, **2014**,**43**:5815-5840
- [4] Li C P, Wang S, Guo W, et al. *Chem. Commun.*, **2016**,**52**: 11060-11063
- [5] Yang X G, Yan D P. *Adv. Opt. Mater.*, **2016**,**4**:897-905
- [6] Li B, Wen H M, Cui Y, et al. *Adv. Mater.*, **2016**,**28**:8819-8860
- [7] Zhang Y, Yuan S, Day G, et al. *Coord. Chem. Rev.*, **2018**,**354**: 28-45
- [8] Cui Y, Yue Y, Qian G, et al. *Chem. Rev.*, **2011**,**112**:1126-1162
- [9] Yu Y, Yue C, Lin X, et al. *ACS Appl. Mater. Interfaces*, **2016**,**8**:3992-3999
- [10] Horcajada P, Gref R, Baati T, et al. *Chem. Rev.*, **2012**,**112**: 1232-1268
- [11] Zheng H, Zhang Y, Liu L, et al. *J. Am. Chem. Soc.*, **2016**, **138**:962-968
- [12] Fan J, Sun W Y, Okamura T, et al. *Inorg. Chem.*, **2003**,**42**: 3168-3175
- [13] Ma L F, Wang Y Y, Liu J Q, et al. *CrystEngComm*, **2009**, **11**:1800-1802
- [14] Su K, Jiang F L, Qian J J, et al. *Inorg. Chem.*, **2013**,**52**: 3780-3786

- [15] Luo J H, Jiang F L, Wang R H, et al. *Inorg. Chem. Commun.*, **2004**, **7**:638-642
- [16] Zhang M L, Wang J J, Ma Z Z, et al. *New J. Chem.*, **2017**, **41**:12139-12146
- [17] Zhang M L, Zheng Y J, Ma Z Z, et al. *Polyhedron*, **2018**, **146**: 180-186
- [18] Sheldrick G M. *Acta Crystallogr. Sect. A: Found. Crystallogr.*, **2008**, **64**:112-122
- [19] Deilami A B, Salehi M, Arab A. *Inorg. Chim. Acta*, **2018**, **476**:93-100
- [20] Lim I T, Choi K Y. *Molecules*, **2013**, **18**:6608-6619
- [21] WANG Qin-Hua(王庆华), YU Li-Li(于丽丽), LIU Qi(刘琦), et al. *Chinese J. Inorg. Chem.*(无机化学学报), **2011**, **27**: 989-995